INTERNATIONAL JOURNAL FOR NUMERICAL METHODS IN FLUIDS, VOL. 5, 225–244 (1985)

A CRITICAL EVALUATION OF SEVEN DISCRETIZATION SCHEMES FOR CONVECTION–DIFFUSION EQUATIONS

M. K. PATEL, N. C. MARKATOS AND M. CROSS

Faculty of Technology, School of Mathematics, Statistics and Computing, Thames Polytechnic, London SE 18 6PF, U.K.

SUMMARY

A comparative study of seven discretization schemes for the equations describing convection–diffusion transport phenomena is presented. The (differencing) schemes considered are the conventional central- and upwind-difference schemes, together with the Leonard,[1] Leonard upwind[1] and Leonard super upwind difference[1] schemes. Also tested are the so called locally exact difference scheme[2] and the quadratic-upstream difference scheme.[3,4] In multidimensional problems errors arise from 'false-diffusion' and function approximations. It is asserted that false diffusion is essentially a multidimensional source of error. No mesh constraints are associated with errors in function approximation and discretization. Hence errors associated with discretization only may be investigated via one-dimensional problems. Thus, although the above schemes have been tested for one- and two-dimensional flows with sources, only the former are presented here. For 1D flows, the Leonard super upwind difference scheme and the locally exact scheme are shown to be far superior in accuracy to the others at all Peclet numbers and for most source distributions, for the test cases considered. Furthermore, the latter is shown to be considerably cheaper in computational terms than the former. The stability of the schemes and their CPU time requirements are also discussed.

KEY WORDS Convection–Diffusion Differencing Schemes Discretization Errors False Diffusion Upwind Scheme Higher Order Schemes Accuracy Stability Computational Cost

INTRODUCTION

The simulation of fluid-flow and heat/mass-transfer phenomena requires the numerical solution of the Navier–Stokes, energy- and species-conservation equations. These equations involve terms describing the time dependence, convection, diffusion and any sources present. The numerical solutions involve the use of interpolation assumptions, for the variation of the fluid properties and their gradients between discrete points on a computational 'grid' that covers the domain of interest. Unless very unwisely done, the interpolation assumptions will not affect the final solution, provided that sufficiently fine grids are used. They do, however, affect the solution when coarse grids are used; this being particularly so for the interpolation of the convection term. For multi-dimensional, multi-phase flow phenomena, involving 2 and 3 space dimensions and two or more sets of equations,[5–7] the power of even present day computer capacity and speed generally proves to be the limiting factor in the use of very fine grids. Therefore, interpolation schemes for the convection terms are required that are sufficiently accurate to permit the performance of complex calculations within presently available computing resources. Computational fluid mechanics has recently experienced several controversies that have, regrettably, delayed its progress considerably. Most of the controversies arose because of the failure to inject physical considerations into the abstract mathematical laws and manipulations.[11] One of the main controversies relates to the so-called 'false diffusion', that is commonly attributed in the literature to the order of accuracy of the

0271–2091/85/03 0225–20$02.00

Received 2 December 1983
Revised 6 April 1984

differencing scheme used. However, the central-difference scheme has second-order accuracy and yet for large Peclet numbers performs less satisfactorily than the upwind scheme which is only first-order accurate. Of course, the upwind scheme overestimates diffusion at large values of Peclet number but this is also true for all other schemes. False diffusion is not governed by the order of the scheme; for steady-state, uniform flow in a co-ordinate direction the first-order upwind scheme has no false diffusion![11] False diffusion exists only in multi-dimensional phenomena and arises because of the common practice of treating the flow across each control-cell face as locally one-dimensional. Therefore schemes that would give less false diffusion should take account of the local multi-dimensional nature of the flow. Such schemes exist[8,9] but it is not the purpose of this work to test them at this time. The true merit of the higher-order schemes is that they approximate better the fluid-property space variation, which is in reality non-linear; so they may be more accurate for relatively coarse grids. The purpose of this work is to test several of the available schemes with a view to evaluating their relative accuracy *vis-à-vis* their generality, stability and computer requirements.

The schemes tested are: the central-difference scheme (CDS); the upwind-difference scheme (UDS); the more complex Leonard, Leonard upwind and Leonard super upwind difference schemes (LDS, LUDS, LSUDS OR LSU); the locally exact difference scheme (LEDS); and the quadratic upstream difference scheme (QUDS) of Leonard[3] as modified by Pollard and Siu.[10]

In Section 2, the general governing equations encountered in fluid-flow problems are outlined. In Section 3, the test problems are introduced, together with their analytic solution. Section 4 outlines the finite-difference equations using the control-volume formulation.[11] Section 5 outlines the nature of the influence coefficients and the restrictions imposed upon the convergence of the schemes. Section 6 briefly outlines the solution procedure. Section 7 introduces the particular test cases used. Section 8 presents the results for the test cases under consideration. Section 9 discusses the results, performance of the schemes and their consequences. Finally, Section 10 presents the concluding remarks of the present study. Since the LEDS and LSUDS may not be familiar to some readers, they are discussed in some detail, and their derivations are given in Appendices I and II.

2. THE TRANSPORT EQUATIONS

Fluid dynamics and heat/mass transfer problems of engineering interest are modelled by the Navier–Stokes and conservation equations. A major convenience for the numerical formulation is provided by the recognition that these equations have a common form.[11] Thus the general steady-state convection–diffusion equation may be written as

$$\frac{\partial}{\partial x_i}(\rho u_i \phi) = \frac{\partial}{\partial x_i}\left(\Gamma \frac{\partial \phi}{\partial x_i}\right) + S \tag{1a}$$

where the dependent variable is denoted by ϕ. The mass flow rate ρu_i appearing in equation (1a) must satisfy an additional equation, the continuity equation for the flow field, written for steady flows as

$$\frac{\partial}{\partial x_i}(\rho u_i) = 0 \tag{1b}$$

The diffusion coefficient Γ represents fluid properties such as conductivity or viscosity, and u_i denotes the velocity in the x_i-direction with ρ being the density. The term on the left-hand side of equation (1) is the convection term, which represents the flux of ϕ convected by the mass flow rate ρu_i. The first term on the right-hand side is the diffusion term and S represents the source term, which could also include any other terms that are not conveniently represented by convection and diffusion terms of the above form. The dependent variable ϕ stands for a variety of physical quantities, such as velocity components, enthalpy, mass fraction etc.; and, depending on ϕ, the Γs and Ss are appropriately expressed.

3. THE TEST PROBLEM

In the introduction we asserted that the order of the discretization scheme only influences the accuracy of the approximation method. This means that the effectiveness of such schemes can be assessed by simple linear problems in one space dimension.

The one-dimensional problem considered has the form

$$\frac{\mathrm{d}}{\mathrm{d}x}(\rho u\phi) = \frac{\mathrm{d}}{\mathrm{d}x}\left(\Gamma\frac{\mathrm{d}\phi}{\mathrm{d}x}\right) + S(x), \quad 0 \leqslant x \leqslant 1 \tag{2a}$$

where ρ, u and Γ are constant without loss of generality; $S(x)$ is a source term and the boundary conditions are of the form

$$\phi(0) = 0; \quad \phi(1) = 1 \tag{2b}$$

The Peclet number for the flow is represented by $P(=\rho u/\Gamma)$. For the purpose of the tests a quadratic source term $S(x) = ax^2 + bx + c$ was assumed, where a, b and c are constants. The analytic solution $\phi(x)$ for the problem depicted by equation (2a), which is characterized by a viscous boundary layer of thickness $1/P$, is

$$\Phi(x) = \frac{Z[\exp(Px) - 1]}{[\exp(P) - 1]} + E \tag{3a}$$

$$\left.\begin{aligned} E &= a'x^3 + b'x^2 + c'x \\ Z &= 1 - a' - b' - c' \\ a' &= a/(3P) \\ b' &= b/(2P) + a/(P^2) \\ c' &= c/P + b/(P^2) + 2a/(P^3) \end{aligned}\right\} \tag{3b}$$

4. FINITE-DIFFERENCE APPROXIMATIONS

For a uniform grid of length Δx, a simple central-difference approximation for the diffusion term is (Figure 1)

$$\left(\frac{\mathrm{d}^2\phi}{\mathrm{d}x^2}\right)_{\mathrm{P}} = \frac{\phi_{\mathrm{E}} - 2\phi_{\mathrm{P}} + \phi_{\mathrm{W}}}{\Delta x^2} \tag{4}$$

which is in general a good approximation, since it is 'third order consistent'.[12] However, it is not the diffusion term approximation that poses the problem, but rather the convection term. In the current contribution we examine seven distinct approximations of the convection term to evaluate their accuracy and practicability for implementation.

The schemes are (see Figure 1 for definitions of points E, W, P, EE etc.):

(i) the central-difference scheme (CDS)

$$\left(\frac{\mathrm{d}\phi}{\mathrm{d}x}\right)_{\mathrm{P}} = \frac{\phi_{\mathrm{E}} - \phi_{\mathrm{W}}}{2\Delta x} \tag{5}$$

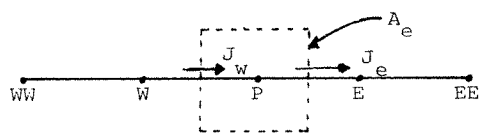

Figure 1. Control volume representation

(ii) the upwind-difference scheme (UDS)

$$\left.\begin{aligned} u>0, \left(\frac{\mathrm{d}\phi}{\mathrm{d}x}\right)_{\mathrm{P}} &= \frac{\phi_{\mathrm{P}}-\phi_{\mathrm{W}}}{\Delta x} \\ u<0, \left(\frac{\mathrm{d}\phi}{\mathrm{d}x}\right)_{\mathrm{P}} &= \frac{\phi_{\mathrm{E}}-\phi_{\mathrm{P}}}{\Delta x} \end{aligned}\right\} \tag{6}$$

(iii) the Leonard difference scheme (LDS)

$$\left.\begin{aligned} u>0, \left(\frac{\mathrm{d}\phi}{\mathrm{d}x}\right)_{\mathrm{P}} &= \frac{\phi_{\mathrm{E}}-\phi_{\mathrm{W}}}{2\Delta x} - \frac{\phi_{\mathrm{E}}-3\phi_{\mathrm{P}}-3\phi_{\mathrm{W}}-\phi_{\mathrm{WW}}}{6\Delta x} \\ u<0, \left(\frac{\mathrm{d}\phi}{\mathrm{d}x}\right)_{\mathrm{P}} &= \frac{\phi_{\mathrm{E}}-\phi_{\mathrm{W}}}{2\Delta x} - \frac{\phi_{\mathrm{EE}}-3\phi_{\mathrm{E}}+3\phi_{\mathrm{P}}-\phi_{\mathrm{W}}}{6\Delta x} \end{aligned}\right\} \tag{7}$$

(iv) the Leonard upwind difference scheme (LUDS)

$$\left.\begin{aligned} u>0, \left(\frac{\mathrm{d}\phi}{\mathrm{d}x}\right)_{\mathrm{P}} &= \frac{11\phi_{\mathrm{P}}-18\phi_{\mathrm{W}}+9\phi_{\mathrm{WW}}-2\phi_{\mathrm{WWW}}}{6\Delta x} \\ u<0, \left(\frac{\mathrm{d}\phi}{\mathrm{d}x}\right)_{\mathrm{P}} &= \frac{2\phi_{\mathrm{EEE}}-9\phi_{\mathrm{EE}}+18\phi_{\mathrm{E}}-11\phi_{\mathrm{P}}}{6\Delta x} \end{aligned}\right\} \tag{8}$$

(v) the Leonard super upwind difference scheme (LSUDS)

$$\left.\begin{aligned} u>0, \left(\frac{\mathrm{d}\phi}{\mathrm{d}x}\right)_{\mathrm{P}} &= \lambda\left(\frac{\phi_{\mathrm{E}}-\phi_{\mathrm{W}}}{2\Delta x} - \frac{\phi_{\mathrm{E}}-3\phi_{\mathrm{P}}+3\phi_{\mathrm{W}}-\phi_{\mathrm{WW}}}{6\Delta x}\right) \\ &\quad + (1-\lambda)\left(\frac{11\phi_{\mathrm{P}}-18\phi_{\mathrm{W}}+9\phi_{\mathrm{WW}}-2\phi_{\mathrm{WWW}}}{6\Delta x}\right) \\ u<0, \left(\frac{\mathrm{d}\phi}{\mathrm{d}x}\right)_{\mathrm{P}} &= \lambda\left(\frac{\phi_{\mathrm{E}}-\phi_{\mathrm{W}}}{2\Delta x} - \frac{\phi_{\mathrm{EE}}-3\phi_{\mathrm{E}}+3\phi_{\mathrm{P}}-3\phi_{\mathrm{W}}}{6\Delta x}\right) \\ &\quad + (1-\lambda)\left(\frac{2\phi_{\mathrm{EEE}}-9\phi_{\mathrm{EE}}+18\phi_{\mathrm{E}}-11\phi_{\mathrm{P}}}{6\Delta x}\right) \end{aligned}\right\} \tag{9}$$

(vi) the locally exact difference scheme (LEDS)

$$\left(\frac{\mathrm{d}\phi}{\mathrm{d}x}\right)_{\mathrm{P}} = \frac{\exp(PP_{\mathrm{e}})-\exp(PP_{\mathrm{w}})}{\Delta x(\exp(P)-1)} \tag{10}$$

Table I. Truncation errors for the differencing schemes, for $S(x)=0$

	Derivatives itemized by equation							
	4	5	6	7	8	9	10	11
Truncation error	$\phi_{\mathrm{P}}^{\mathrm{IV}}$	$\phi_{\mathrm{P}}^{\mathrm{III}}$	$\phi_{\mathrm{P}}^{\mathrm{II}}$	$\phi_{\mathrm{P}}^{\mathrm{IV}}$	$\phi_{\mathrm{P}}^{\mathrm{IV}}$	$\phi_{\mathrm{P}}^{\mathrm{IV}}$		$\phi_{\mathrm{P}}^{\mathrm{IV}}$
Principal part	Δx^2	Δx^2	Δx	Δx^3	Δx^3	$(4\lambda-3)\Delta x^3$		Δx^3
Scheme	CDS	CDS	UDS	LDS	LUDS	LSUDS	LEDS	QUDS

(vii) the quadratic upstream difference scheme (QUDS) at the east cell-face;

$$\left.\begin{aligned} u>0, \quad \phi_e &= \tfrac{1}{2}(\phi_P+\phi_E)-\tfrac{1}{8}(\phi_W-2\phi_P+\phi_E) \\ u<0, \quad \phi_e &= \tfrac{1}{2}(\phi_P+\phi_E)-\tfrac{1}{8}(\phi_{EE}-2\phi_E+\phi_P) \end{aligned}\right\} \tag{11}$$

The truncation errors for these discretization schemes are tabulated in Table I when $S(x)=0$.

5. METHOD OF FORMULATION AND INFLUENCE COEFFICIENTS

The general equation (1) is integrated over the control volume in Figure 1, with P as the central node and E, W, its neighbours. The corresponding faces of the control volume are denoted by e and w. The above notation is conventional.[11,13]

The finite-difference equation is represented by

$$J_e A_e - J_w A_w + \bar{S}\Delta x = 0 \tag{12}$$

over the control volume shown in Figure 1, where $\Delta x \times 1 \times 1$ is its volume and $\bar{S}$ is the average source term within the control volume. A_j are the cell-face areas.

It is to be noted that the implied conservatism of the differencing schemes is a strong desideratum. Substitution of the various convection derivatives (i.e. expressions (5)–(11)) and the diffusion derivative (expression (4)) in equation (12) leads to the final discretized equation which has the form

$$a_P\phi_P = \Sigma a_{nb}\phi_{nb} + b \tag{13}$$

where the subscript nb denotes the neighbours of the grid point P, and b denotes contributions from source terms. On defining the mesh Peclet number by

$$P_i = C_i/D_i = \rho u_i \Delta x/\Gamma \tag{14a}$$

where

$$C_i = \rho u_i; \quad D_i = \Gamma/\Delta x \tag{14b}$$

one can express the influence coefficients a_i in a simple and more meaningful way,[11] as shown in Table II, where $[c1, c2]$ denotes the maximum of the variables $c1$ and $c2$, and subscript u denotes 'upstreams'.

The main points to be noted in Table II are (a) the CDS influence coefficients become negative if $C > 2D$, and this would in turn lead to oscillatory and non-convergent solution.[11] One way of overcoming this problem is to use finer grids, but in practice this is not always feasible owing to high costs; (b) the UDS influence coefficients are always greater than zero, and predict physically plausible solutions at all Peclet numbers; (c) the LDS has two distinct types of influence coefficients but, since the effect of the downstream coefficient is swamped, the restriction on this scheme is

Table II. Influence coefficients

Scheme	a_e^w	a_{ee}^{ww}	a_{eee}^{www}
CDS	$D-C/2+[\pm C,0]$	—	—
UDS	$D+[\pm C,0]$	—	—
LDS	$6D\pm[\mp 2C,0]$	$\mp[C_u,0]$	—
LUDS	$6D\pm[\mp 18C,0]$	$\mp[-9C_u,0]$	$\pm[\pm 2C_{uu},0]$
LSUDS	$\lambda(a_{LDS})+(1-\lambda)(a_{LUDS})$	$\lambda(a_{LDS})+(1-\lambda)(a_{LUDS})$	$(1-\lambda)(a_{LUDS})$
LEDS	$C/(\exp(C/D-1)+[C,0])$	—	—
QUDS	$D\pm[\mp 3C/8,\pm 6C/8]\pm[C/8,0]$	$\mp[\pm C/8,0]$	—

$C > 3D$, the violation of which will lead to oscillatory solutions. In general, however, since all contributions lying outside the immediate neighbours are 'dumped' in the source term, the scheme is computationally viable; (d) the LUDS goes one step further by including a further downstream contribution, thus needing modified representations close to the boundary; (e) the LSUDS is a combination of the LDS and LUDS, where the weighting factor λ is evaluated from a knowledge of the analytic solution. Thus the influence coefficients never become negative; but we do need to evaluate a series of exponential functions, which at times is expensive; (f) the LEDS, termed as 'smart upwind method', is exact for one-dimensional problems with zero source; (g) finally the QUDS of Leonard,[12] does suffer from convergence problems, as will be shown below. However one way of overcoming the convergence problems is to introduce 'pseudo-source' terms such as those by Han and Humphrey.[14] Then one needs to store values at previous iterations, which is not efficient for large practical simulation problems.

6. SOLUTION PROCEDURE

The set of linear algebraic equations (13) was solved using what is known as the Thomas algorithm[15], properly modified for the non-symmetric-banded cases.

7. ONE-DIMENSIONAL TEST CASES

The finite-difference schemes were tested over a wide range of Peclet numbers for eight test cases with zero, linear and quadratic source terms. The number of nodes, N, ranged from 5–100 in steps of 5 for all test cases. Table III presents a summary of the cases considered.

The ranges of Peclet numbers, P, and mesh Peclet numbers, P_e, studied were from $1–10^5$ and $0{\cdot}2–10^3$, respectively, for all cases. The presented sample results for simplicity refer to Peclet numbers and mesh Peclet numbers from 1–100 and 1–50, respectively, since the behaviour for the higher Peclet number cases is the same. As seen in Table III, the following one-dimensional convection–diffusion situations were considered. Test case 1, was the standard 'no source' situation, whereas test case 2 was one with a constant source term. Test cases 3 and 4 had linear source terms with positive and negative gradients, respectively. Test cases 5–8 all had quadratic source terms, with different constants a, b and c.

Table III. One-dimensional test cases considered

Test case	Peclet number $P = \rho u/\Gamma$	Range of mesh Peclet number	Number of nodes	Source term $S(x)$
1	$1–10^5$	$0{\cdot}2–10^3$	5–100	0
2	$1–10^5$	$0{\cdot}2–10^3$	5–100	50
3	$1–10^5$	$0{\cdot}2–10^3$	5–100	x
4	$1–10^5$	$0{\cdot}2–10^3$	5–100	$-x$
5	$1–10^5$	$0{\cdot}2–10^3$	5–100	$x^2 - x - 1$
6	$1–10^5$	$0{\cdot}2–10^3$	5–100	$-x^2 + x - 1$
7	$1–10^5$	$0{\cdot}2–10^3$	5–100	$-x^2 - x + 1$
8	$1–10^5$	$0{\cdot}2–10^3$	5–100	$x^2 + x + 1$

Table IV. Test case results for $P = 20$, $x = 0{\cdot}8$ and $N = 5, 10, 20$

Test case	Equation (3) Exact	Equation (5) CDS	Equation (6) UDS	Equation (7) LDS	Equation (8) LUDS	Equation (9) LSUDS	Equation (10) LEDS	Equation (11) QUDS
	0·0183	−0·3279	0·1997	−0·0753	0·1263	0·0183	0·0183	−0·1154
1	0·0183	0·0000	0·1111	0·0161	0·0583	0·0183	0·0183	0·0102
	0·0183	0·0123	0·0625	0·0201	0·0298	0·0183	0·0183	0·0181
	1·9725	2·4918	1·7004	2·1130	1·8105	1·972	1·972	2·1713
2	1·9725	2·0000	1·8334	1·9758	1·9126	1·972	1·972	1·9845
	1·9725	1·9815	1·9063	1·9698	1·9552	1·972	1·972	1·9729
	0·0358	−0·3009	0·2153	−0·0553	0·1408	0·0358	0·0379	−0·0921
3	0·0358	0·0180	0·1278	0·0337	0·0747	0·0358	0·0364	0·0283
	0·0358	0·0300	0·0797	0·0375	0·0470	0·0358	0·0360	0·0357
	0·0008	−0·3549	0·1842	−0·0954	0·1118	0·0008	0·0013	−0·1387
4	0·0008	−0·0180	0·0944	−0·0014	0·0419	0·0008	0·0002	−0·0079
	0·0008	0·0053	0·0453	0·0027	0·0127	0·0008	0·0007	0·0005
	−0·0283	−0·3953	0·1637	−0·1275	0·0859	−0·028	−0·028	−0·1707
5	−0·0283	−0·0478	0·0699	−0·0306	0·0140	−0·028	−0·028	−0·0372
	−0·0283	−0·0346	0·0185	−0·0264	−0·0161	−0·028	−0·028	−0·0286
	−0·0132	−0·3732	0·1758	−0·1107	0·0994	−0·013	−0·013	−0·1516
6	−0·0132	−0·0322	0·0834	−0·0155	0·0284	−0·013	−0·013	−0·0214
	−0·0132	−0·0194	0·0328	−0·0114	−0·0012	−0·013	−0·013	−0·0134
	0·0299	−0·3144	0·2048	−0·0633	0·1377	0·030	0·026	−0·1067
7	0·0299	0·0118	0·1190	0·0278	0·0698	0·030	0·029	0·0213
	0·0299	0·0240	0·0721	0·0317	0·0414	0·030	0·030	0·0296
	0·0849	−0·2285	0·2547	0·0001	0·1823	0·0848	0·0889	−0·0326
8	0·0849	0·0682	0·1721	0·0829	0·1209	0·0849	0·0860	0·0781
	0·0849	0·0794	0·1266	0·0865	0·0953	0·0849	0·0852	0·0848

8. PRESENTATION OF RESULTS

The main results are presented in Table IV and Figures 2–14. Table IV summarizes the results for each scheme under consideration, for $P = 20$.

In all Figures presented, the accompanying table summarizes the important characteristics such as maximum error, evaluated as $\max(|\Phi_i - \phi_i|/\Phi_N)$, the error norm evaluated by $(\sum(|\Phi_i - \phi_i|)^2)^{1/2}$ and finally, the predicted flux at the outflow boundary (Φ_N), evaluated by

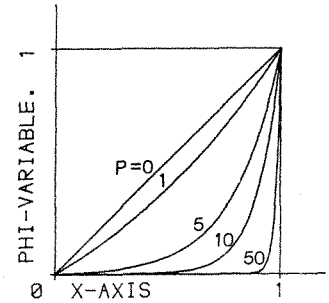

Figure 2. Analytic solution of the one-dimensional, zero source problem for $P = 0$, 1, 5, 10 and 50

	EAS	CDS	UDS	LUD	LDS	LSU	LED
MAX-ERROR		0.509	0.091	0.053	0.073	0.	0.
ERROR NORM		0.767	0.091	0.053	0.231	0.	0.
FLUX AT X=1	-7.500	-13.500	-6.612	-6.975	-9.870	-7.500	-7.500

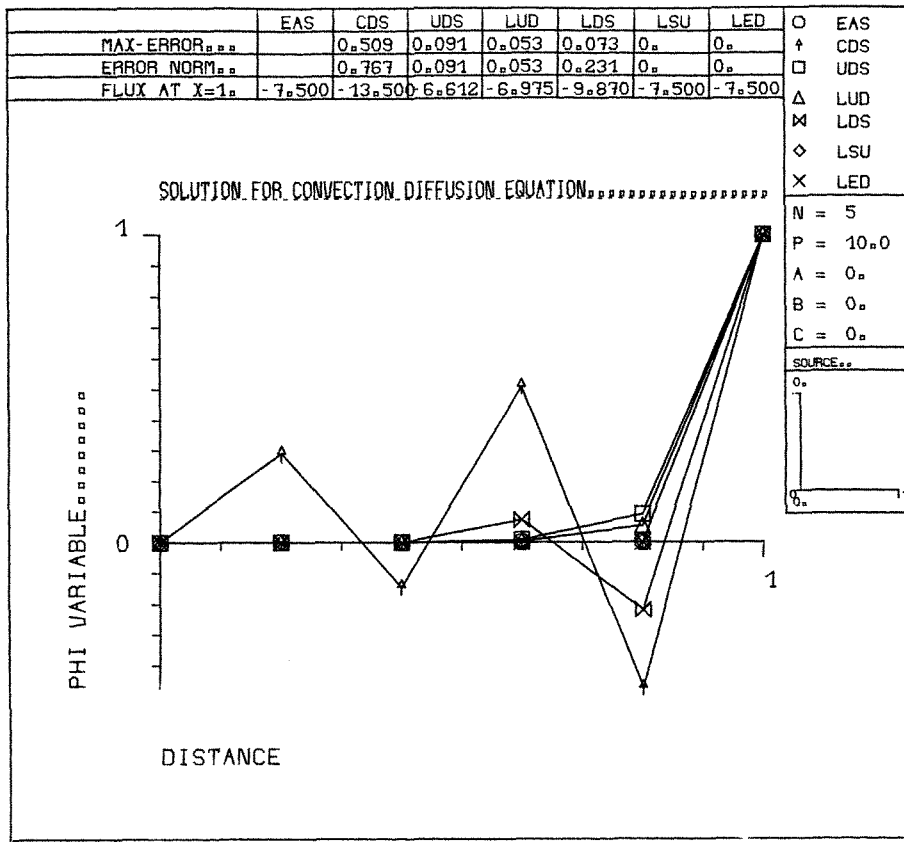

Figure 3. Numerical solution for zero source

	EAS	CDS	UDS	LUD	LDS	LSU	LED
MAX-ERROR...		0.019	0.138	0.	0.009	0.	0.128
ERROR NORM..		0.031	0.202	0.002	0.009	0.	0.175
FLUX AT X=1.	-1.740	-1.500	-0.653	-1.761	-1.645	-1.740	-0.700

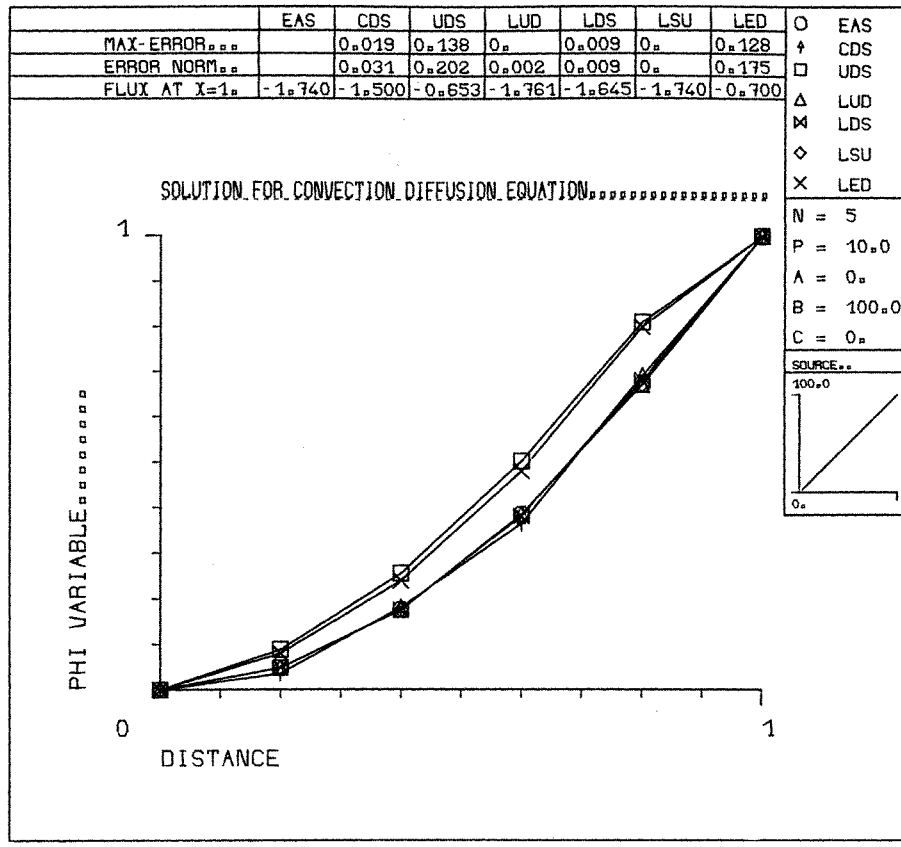

Figure 4. Numerical solution for linear, positive gradient, source

	EAS	CDS	UDS	LUD	LDS	LSU	LED
MAX-ERROR...		0.265	0.136	0.083	0.029	0.	0.
ERROR NORM..		0.609	0.125	0.071	0.174	0.	0.001
FLUX AT X=1.	-12.07	-21.61	-9.96	-10.77	-14.96	-12.07	-12.08

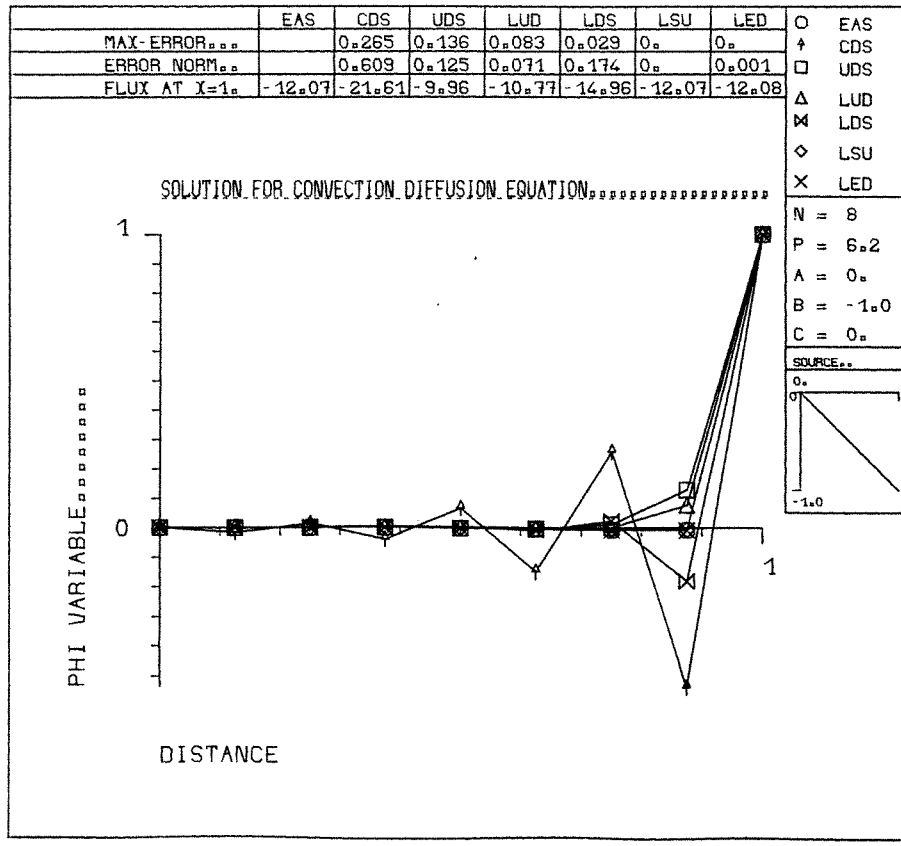

Figure 5. Numerical solution for linear, negative gradient, source

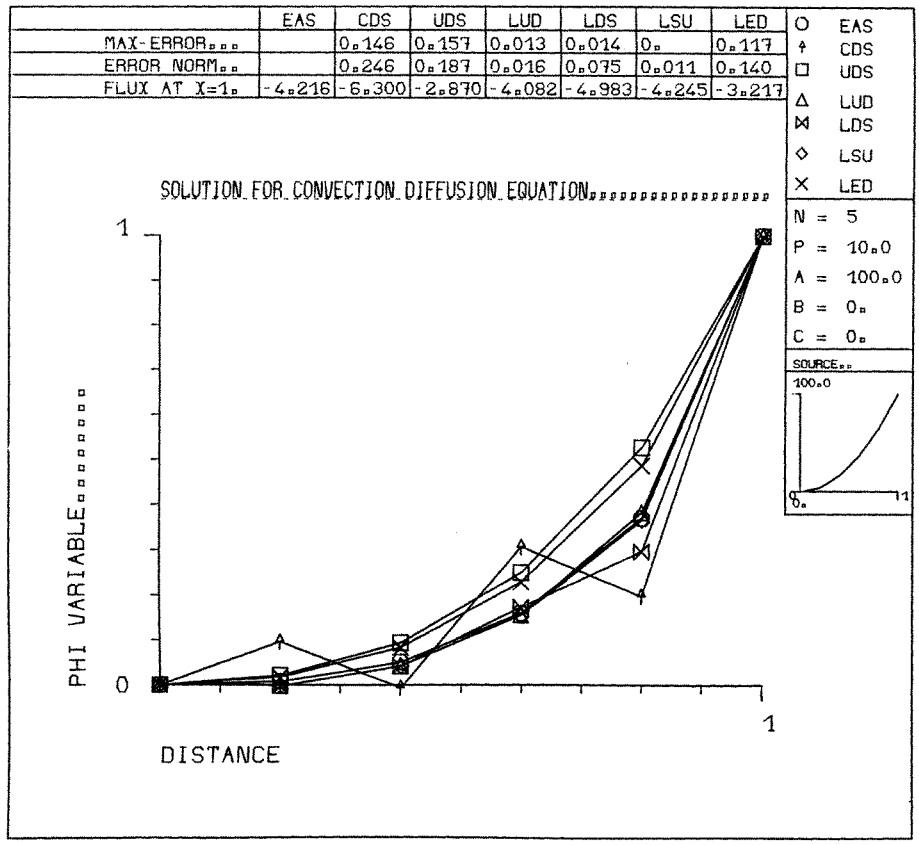

Figure 6. Numerical solution for quadratic, positive gradient, source

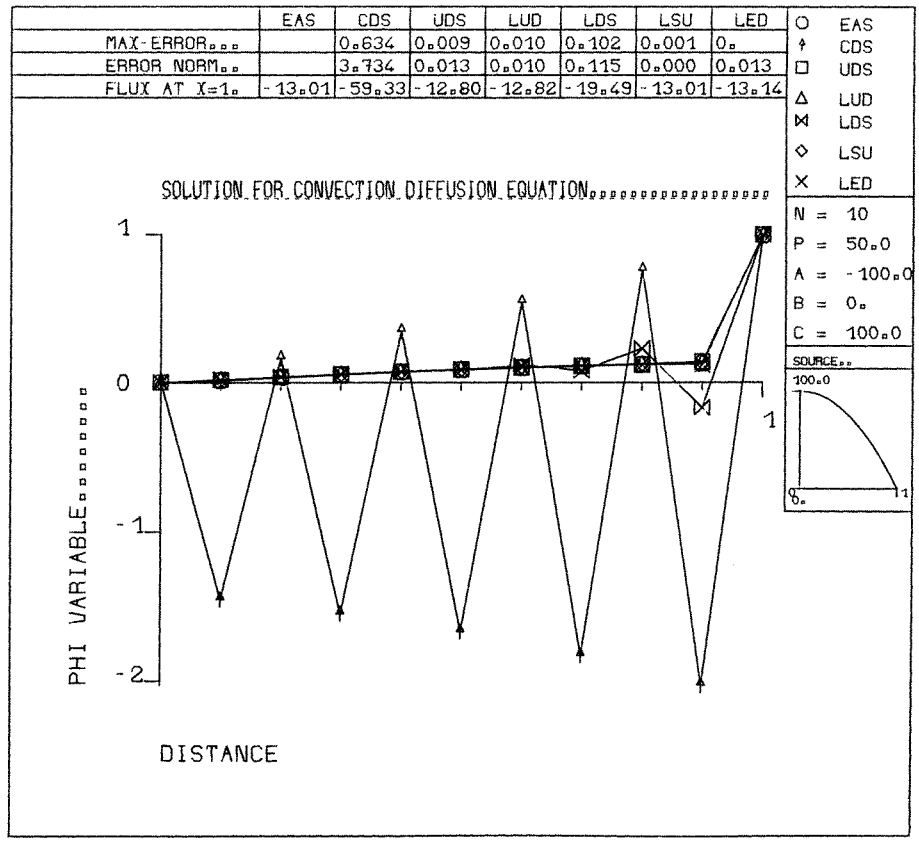

Figure 7. Numerical solution for quadratic, negative gradient, source

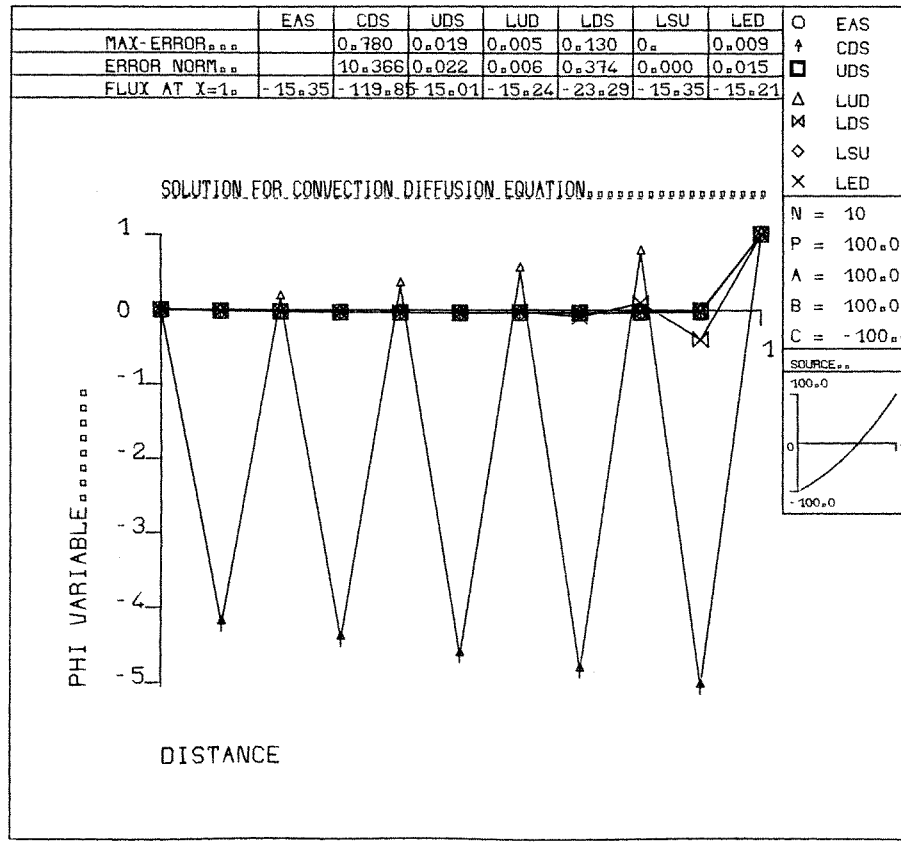

Figure 8. Numerical solution for large sources, details on graph

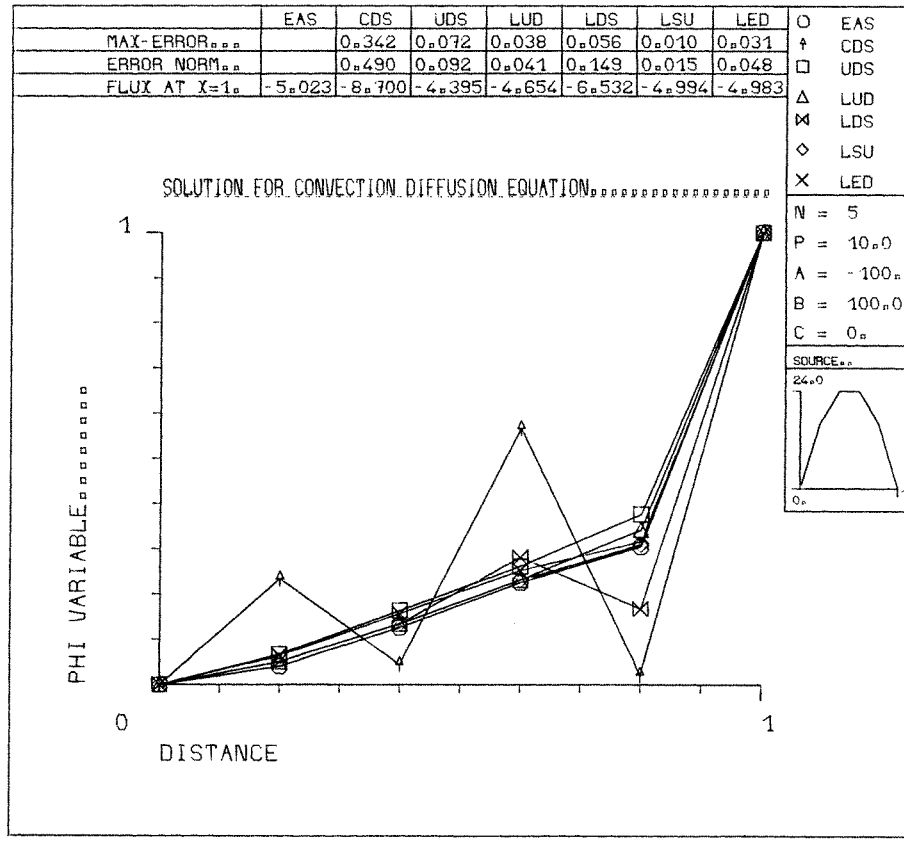

Figure 9. Numerical solution for large sources, details on graph

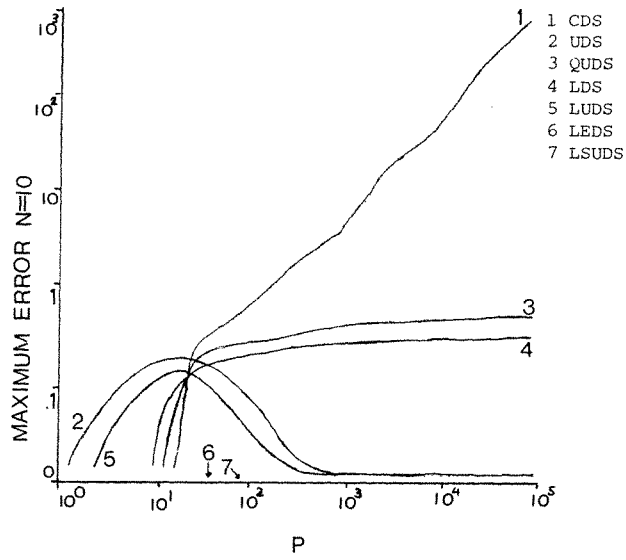

Figure 10. Plot of maximum error versus Peclet number for $N = 10$

$-(\phi_{N-2} - 4\phi_{N-1} + 3\phi_N)/(2\Delta x)$, for the finite-difference schemes, and by $-(ZP\mathrm{e}^P)/(\mathrm{e}^P - 1) + 3a'x^2 + b'x + c'$ for the exact solution.

Figure 2 represents the analytic behaviour of ϕ for several Peclet numbers for the cases with zero source.

Figure 3 compares the solutions obtained by the various schemes for the test case with zero source against the analytic solution.

Figures 4 and 5 compare the results of the various schemes for the cases with a linear source term with positive and negative gradients, respectively.

Figures 6 and 7 compare the results of the various schemes for the cases with a quadratic source term with positive and negative gradients, respectively.

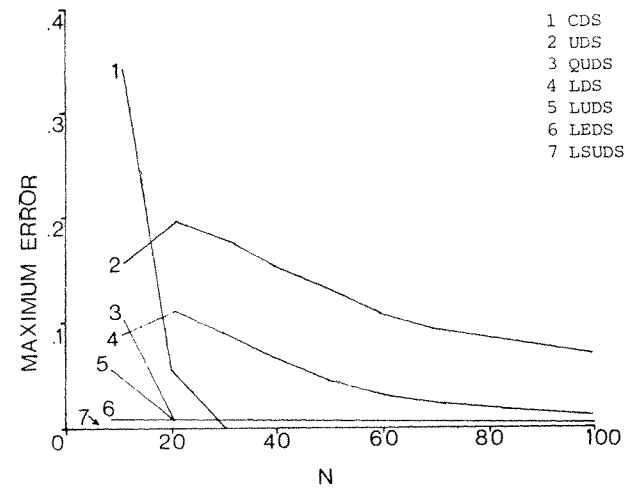

Figure 11. Plot of maximum error versus number of nodes for $S(x) = x^2 + x + 1$

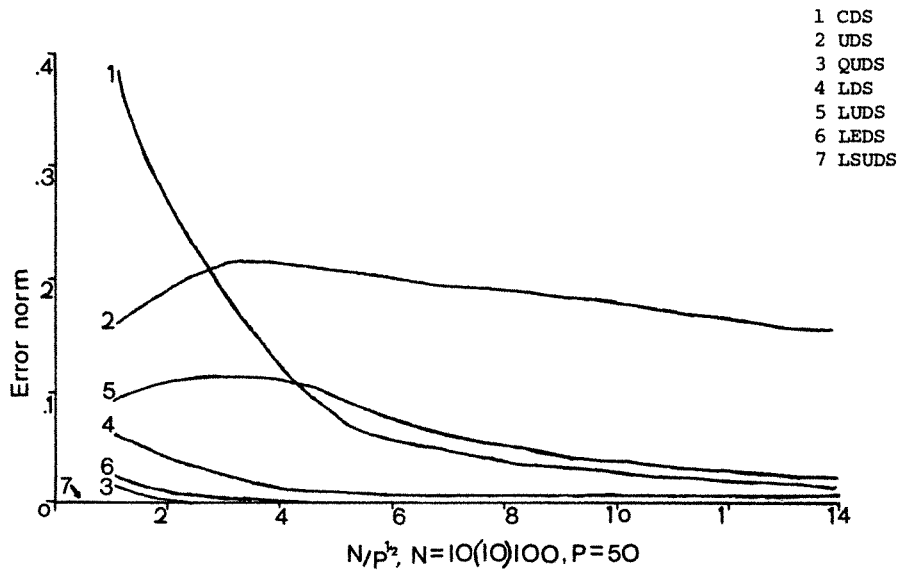

Figure 12. Plot of error norm versus $N/P^{1/2}$ for $P = 50$ and N ranging from 1 to 100 in steps of 10

Figures 8 and 9 compares the performance of the schemes for cases with large source terms, generated by the expressions for test cases 5–8, in Table III.

Figures 10 to 13 present typical maximum error profiles as functions of the number of nodal points used, for all schemes tested; and Figure 14 presents the computational requirements in terms of CPU seconds on the Prime series 750 computer.

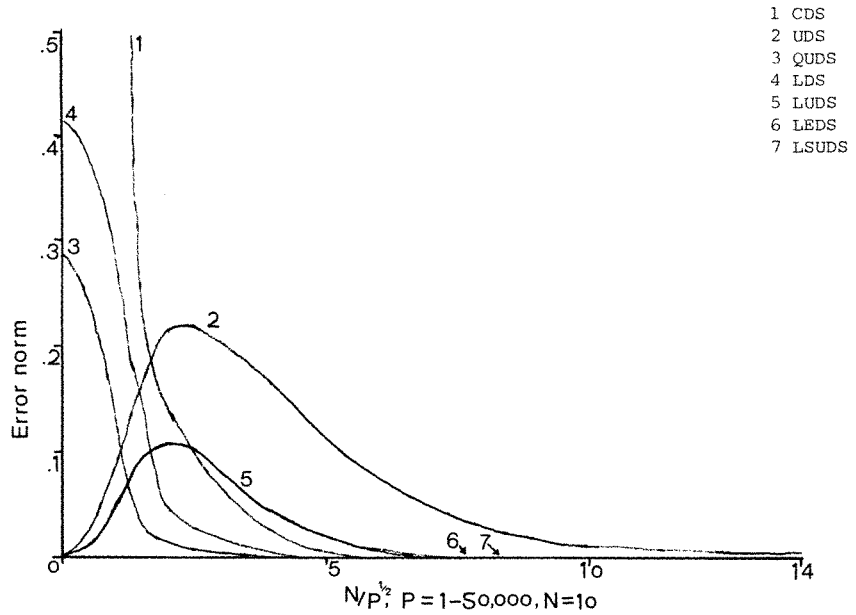

Figure 13. Plot of error norm versus $N/P^{1/2}$ for $N = 10$ and P ranging from 1 to 50,000

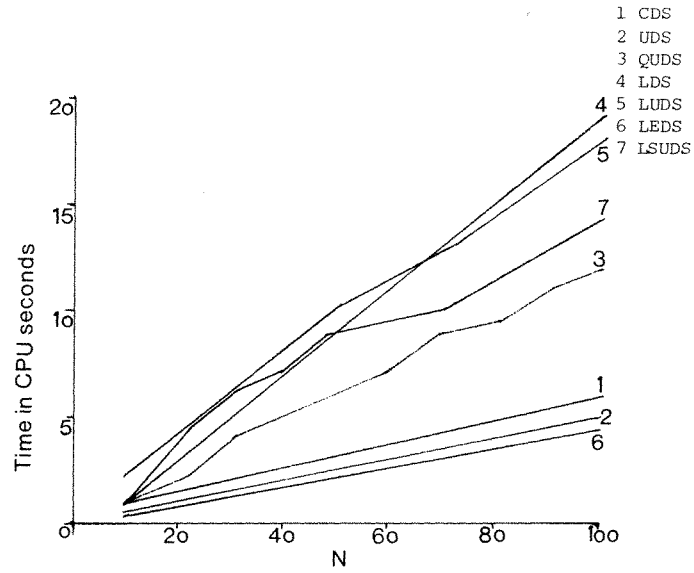

Figure 14. Plot of CPU seconds versus number of nodes for $S(x) = -x$

9. DISCUSSION OF RESULTS

Figure 2 clearly depicts the viscous boundary layer, where the solution, $\phi(x)$, rapidly changes from $\phi(0)$ to $\phi(1)$. The curves for large Peclet numbers do not vary considerably within the first $(N-2)$ nodal points for $P > 0$.

Figure 3 depicts an oscillatory behaviour of the CDS solution and indicates that the UDS overpredicts the nodal ϕ-values further downstream of the 70 per cent station. Inspection of the results reveals that the UDS is inaccurate even for moderate Peclet numbers, unless the grid is sufficiently fine; but that it does predict qualitatively realistic solutions, unlike the 'wiggles' of the CDS. The LDS and the LUDS solutions are not much of an improvement, the former being also oscillatory. In contrast, the LSUDS and the LEDS are seen to be in excellent agreement with the analytical solution, throughout the domain.

Figures 4 and 5 correspond to the linear source cases, and indicate again that both the CDS and the LDS solutions are oscillatory in nature. The other comments relating to the case with zero source (Figure 3) are also valid, the UDS overpredicting ϕ downstream, and the LSUDS and the LEDS solutions being very accurate over the whole domain.

Figures 6 and 7 correspond to the quadratic source cases, and indicate that both the CDS and LDS are once again oscillatory.

Figures 8 and 9 correspond to the large source cases, and clearly depict the unboundedness in the oscillatory nature of the CDS, whereas they indicate that LEDS predicts very good results. The LDS appears to predict oscillatory results within the last few nodal points.

Inspection of Figures 3 to 9 reveals that, in general, all the test cases were well modelled by both the LEDS and the LSUDS with errors of $\max(|\Phi_i - \phi_i|/\Phi_N)$ less than 10^{-6}, for all Peclet numbers. However, considerable errors are indicated when using the LEDS for very large source terms. The CDS performed well for mesh Peclet number less than 2, but was grossly in error for higher Peclet numbers, for both test case 1 (with zero source, Figure 3) and when the type of source, $S(x)$, did not affect the outcome to a great extent (i.e. when the source and solution profiles are similar in shape,

Figure 4). Inspection of Table IV reveals that wiggles are predicted by the CDS, whereas the UDS, although always stable, is in considerable error at all flow rates and practical mesh sizes. The results indicate that the UDS always overestimated the solution by at least 15 per cent, even for relatively fine grids, whereas the QUDS underpredicted the solution by only a few per cent. The LEDS appeared to overestimate the solution for the problems with large source terms by around 5 per cent at the extreme, whereas the LSUDS was within 0·01 per cent for all test cases considered, including those with large source terms. This is expected since the exact solution is a combination of an exponential and a cubic, in which case the LSUDS is 'exact', except for inaccuracies arising near boundaries. Also indicated in Table IV are the wiggles in the solutions obtained by the LDS and QUDS, owing to the ill-conditioned influence coefficients.

It is clear from the above Figures and Tables IV that the LSUDS and the LEDS give by far the most accurate solutions, as expected. However, before any judgement can be formulated about the relative performance of the schemes, it is important to compare the profiles of the maximum errors both as functions of the mesh size and of the Peclet number, and with respect to the computational requirements for the schemes. After all, if a scheme is convergent, a more accurate solution may always be obtained by mesh refinement, until round-off error dominate truncation error. Therefore, it is the authors opinion that accuracy should be compared on the basis of relative CPU and storage costs together with convenience of programming effort. This information is provided by Figures 10–14.

Figure 10 presents the behaviour of the maximum error with increasing Peclet number (from $P = 10^0$ to 10^5) for a constant grid size ($\Delta x = 0{\cdot}1$). The profiles shapes for the UDS and LUDS are similar and those for the LDS and QUDS are also similar. The CDS error profile diverges as the Peclet number increases. The LEDS and LSUDS profiles are not depicted in Figure 10 as they lie close to the P-axis.

Figure 11 shows that there exists a critical region of the mesh size, over which the UDS error is maximum (being from $N = 15$ to $N = 40$ for this particular case). Outside this region the maximum error does not increase with decrease in mesh size. It is interesting to observe that for the UDS the error profile flattens out very slowly. The number of nodal points, N, required to obtain a given accuracy by the UDS is nearly three times that of the LDS (e.g. LDS requires $N = 30$ and UDS requires $N = 80$ for this particular case).

Figures 12 and 13 depict the maximum error profiles versus $N/P^{1/2}$ for constant P and constant N, respectively; the range of N for the former being between 10 and 100 and the range of P, for the latter, being between 10^0 and 5×10^4. The error profiles for increasing P indicate that the maximum errors tend to zero for both UDS and LUDS, but that they tend towards a limiting value, considerably greater than zero, for the QUDS and LDS (for this particular case). The profiles for the LEDS and LSUDS are not presented, as they lie close to the $N/P^{1/2}$-axis in Figure 13.

Figure 14 shows crude computational requirements in CPU seconds, on a PRIME series 750 computer. It is seen that the time requirements for the LDS are about three times those for the UDS. This is true in general, so that for a given accuracy (up to a limit) the UDS is marginally cheaper than the LDS, considering that the former requires less than three times the number of nodes required by the latter for this accuracy. The presented computer time requirements are for obtaining a given accuracy and should not be interpreted as machine accurate because of the limitations in the time print-out. What is established however is that the upwind- and central-difference schemes are the least expensive, as expected, closely followed, as may not be expected, by the locally exact scheme. It should be mentioned in this context that the calculation of the exponentials involved in the latter was reprogrammed by the authors and appeared to be more efficient than the standard PRIME-library calculations. In practice, and to avoid overflow, asymptotic formulae avoiding calculation of exponentials completely would be used for large

exponents in all schemes The LSUDS and the QUDS are both about 2·0 times more expensive than the above three schemes, for the same number of nodal points, and the LDS and LUDS are about 3·0 times more expensive.

10. CONCLUSIONS

A comparative study in terms of accuracy and computer requirements has been presented for seven numerical schemes, which were applied to a series of simple 1D convection–diffusion problems including linear and non-linear sources. One-dimensionality was imposed in order to eliminate the additional complexity of the multi-dimensional 'false-diffusion'.

The main findings may be summarized as follows:

1. The central-difference and Leonard's LD and LUD schemes proved the most unstable. The first two were also inaccurate although they are both second order. This indicates that it is not only the order of the scheme that dictates the accuracy of the solution in convection/diffusion problems, but also the particular formulation which must account for the asymmetric nature of convection.

2. The central and upwind schemes lead to inaccurate solutions for moderate and high Peclet numbers, and for moderate grids. The upwind scheme presents a flat error profile versus number of nodes, for moderately fine grids. There is therefore a danger that moderate grid refinement may indicate as grid-independent a solution which is still in considerable error. Indeed, in order to obtain with the UDS the same accuracy as with the LSUDS the number of nodes had to be increased to 200. Therefore, for grid-independency studies with the UDS a many-fold increase in the number of nodes may be necessary.

3. For moderate grids, the higher order schemes were, in general, more accurate (when convergent!) than the first order upwind scheme. An exception was the CDS for $Pe > 2$ when it became highly inaccurate. However, all the schemes except the central and locally exact schemes were 2·0 to 3·0 times more expensive than the UDS in computational terms.

4. The LSUDS was, as expected, the most accurate scheme, very closely followed by the LEDS and the QUDS. However, the latter was sometimes oscillatory. The LEDS was both accurate and economical. Furthermore the influence coefficients (i.e. g_m and g_p; see Appendix II) of the LEDS can be calculated and tabulated to improve even further the computational requirements.

5. The schemes considered here fall into three categories, in order of increasing demand in terms of computational requirements, as follows:

(a) Central-difference scheme
    Upwind-difference scheme
    Locally exact difference scheme
(b) Leonard super upwind difference scheme
    Quadratic upstream difference scheme
(c) Leonard upwind difference scheme
    Leonard difference scheme.

The CPU times required are compared with the UDS. For the one-dimensional cases considered, the LDS was found to be approximately three times as expensive as the UDS, whereas the accuracy was within 10 per cent, unlike the UDS, which was at least 20 per cent in error. The LSUDS required just about twice the computer time compared to the UDS, but the LSUDS was within 0·01 per cent in error. Finally the LEDS required between 2 and 3 per cent less CPU time for a maximum error of around 5 per cent (because it required much fewer iterations for a given accuracy), which means that the LEDS could prove a very efficient scheme. The combination of the findings of this study on accuracy *vis-a-vis* computer requirements leads to the following general conclusions:

(i) When a 5 per cent average error of the numerical solution at the grid points is acceptable, one might as well use the UDS with fine grids because it is unconditionally stable and convenient in programming effort. The total CPU requirements will be the same as for the most accurate schemes with coarser grids.

(ii) Should a very accurate solution be required then one should abandon the UDS because of its flat error response to further grid refinement, and choose either the QUDS or LSUDS or LEDS. Of those three the first may be unstable, the second is the most accurate and the third the cheapest. The above conclusions are based on the detailed study of a series of linear 1D problems with linear and non-linear sources, only. Therefore, the general applicability of these conclusions is by no means established as yet. It is suggested that the LEDS may have not received the attention it deserves from the computational fluid-dynamics community, and that further research in evaluating and developing it (particularly in 2D and 3D cases, where its application along streamlines would also eliminate multi-dimensional false diffusion) may prove fruitful. Work is currently in progress on 2D problems and will be reported elsewhere.

ACKNOWLEDGEMENT

The authors wish to thank Dr. D. G. Tatchell of CHAM Ltd., London, for fruitful discussions throughout this work.

NOMENCLATURE

a, b, c	quadratic-profile source coefficients
a', b', c'	modified coefficients in source expressions
a_P, a_{nb}	general coefficients for finite-difference equation (a_P coefficient at point P, a_{nb} coefficients at neighbouring points of point P).
e, w	cell-faces of control volume
g_p, g_m	functions defined in Appendix
b	bulk 'source' term
u_i	non-dimensional velocity component in the i-direction
x_i	co-ordinate distance
A_e, A_w	control-volume face area
C_i	convection term $= \rho u_i$
D_i	diffusion term $= \Gamma/\Delta x$
E	modified source term
W, P, E	nodal point (centres of control volumes)
J_e, J_w	fluxes at East and West faces of control volume
L	function defined in Appendix
N	number of grid nodes
P	Peclet number $= \rho u/\Gamma$
P_i, P_e	mesh Peclet number $= C_i/D_i$
S^*	integrated source term
S	source term
$\bar{S}$	average source within control volume
U_i	velocity at ith-control-volume face
Z	modified multiplier
$[c_1, c_2]$	maximum of c_1 and c_2
Δx	mesh size in x-direction.
$\beta, \gamma, \mu, \lambda$	functions defined in Appendix

ξ variable defined in Appendix
Γ_i diffusion coefficient at ith control volume face
λ Leonard super upwind difference scheme weighting factor
Γ non-dimensional diffusion coefficient
ρ density
ϕ non-dimensional dependent variable
Φ analytical solution for dependent variable ϕ

APPENDIX I

Integration of equation (1a) twice gives;

$$\phi = \frac{F}{u} + C_1 e^{u/\Gamma x} \tag{15}$$

assuming that F and u are constant between two adjacent 'nodal' values. Then by evaluating ϕ in (15) for the west face, between i and $i-1$, and eliminating the constant of integration C_1, we get:

$$\frac{\phi - \phi_{i-1}}{\phi_i - \phi_{i-1}} = \frac{\exp(u_w/\Gamma_w(x - x_i)) - 1}{\exp(u_w/\Gamma_w(x_i - x_{i-1})) - 1} \tag{16}$$

where the flux at the west face, J_w, has the form

$$J_w = \frac{u_w(\phi_{i-1} - \phi_i)\exp(-u_w/\Gamma_w \Delta x)}{(1 - \exp(u_w/\Gamma_w \Delta x)} \tag{17}$$

and similarly J_e has the form

$$J_e = \frac{u_e(\phi_{i-1} - \phi_i)\exp(u_e/\Gamma_e \Delta x)}{(1 - \exp(u_e/\Gamma_e \Delta x)} \tag{18}$$

Equations (17) and (18) can be written in a simpler form by introducing two new functions; these being

$$g_p(\xi) = \frac{\xi}{\exp(\xi) - 1}$$

and (19)

$$g_m(\xi) = \frac{-\xi}{\exp(\xi) - 1}$$

thus giving

$$J_w = \Gamma_w(g_m(u_w \Delta x/\Gamma_w)\phi_{i-1} - g_p(u_w \Delta x/\Gamma_w)\phi_i)/\Delta x \tag{20a}$$

and

$$J_e = \Gamma_e(g_m(u_e \Delta x/\Gamma_e)\phi_i - g_p(u_e \Delta x/\Gamma_e)\phi_{i+1})/\Delta x \tag{20b}$$

Finally the finite difference form for equation (1) using the LEDS is

$$J_e - J_w = S^* \tag{21}$$

Note that, as we are interested in the representations of the convection term only, one could use the second order finite difference representation for the second derivative, and the exponential representation for the convection term, i.e. equation (10).

APPENDIX II

Consider equation (9a) together with equation (4) which gives the LSUDS; for $u > 0$ and $P = u/\Gamma$.

$$\frac{P}{6\Delta x}\{\lambda(2\phi_{i+1} + 3\phi_i - 6\phi_{i-1} + \phi_{i-2}) + (1-\lambda)(11\phi_i - 18\phi_{i-1} + 9\phi_{i-2} - 2\phi_{i-3})$$

$$-\frac{1}{h^2}\{(\phi_{i-1} - 2\phi_i + \phi_{i+1}) = L(\phi_i), \quad i \in [3, N-1] \tag{22}$$

together with

$$\phi_0(0) = 0; \quad \phi_N(1) = 1$$

Substituting

$$\phi = \frac{\exp(Px_i) - 1}{\exp(P) - 1} \tag{23}$$

in (22) and simplifying we have

$$\lambda = \frac{6 - (6 + 11P_e)\exp(-P_e) + 7P_e\exp(-2P_e) - 2P_e\exp(-3P_e) - \beta}{2P_e(1 - \exp(-P_e))^3} \tag{24}$$

where

$$\beta = \frac{\Delta x^4}{2}\exp(-P_e) + 2P_e\Delta x^4\exp(-P_e) - 3P_e\frac{\Delta x^4}{2}\exp(-P_e) \tag{25}$$

which, when neglected, is the error introduced in the numerical LSUDS; even then $\beta \ll 1$, so it would be wise to neglect such terms as the scheme is already rather involved. Similar expressions for λ and β can be obtained for $u < 0$.

Modifications at the boundary need the introduction of two further weighting parameters, γ and μ. Once again consider the case $u > 0$ and use the finite-difference representation, for $i = 1$,

$$\frac{P}{2h}(\phi_2 - \phi_0 + \mu_1(\phi_3 - 3\phi_2 + 3\phi_1 - \phi_0)) - \frac{1}{h^2}(\phi_0 - 2\phi_1 + \phi_2) = L_1(\phi_1) \tag{26}$$

which when substituted by equation (23), yields

$$\mu = \frac{\exp(-P_e)((1 - \exp(P_e)) - P_e(1 + \exp(-P_e))/2}{(P_e(1 - \exp(-P_e))^2/2)} \tag{27}$$

Similarly at the 'nodal' point $i = 2$, we use an expression of the form of equation (26), which yields

$$\gamma = \frac{((1 - \exp(-P_e)) - P_e(1 + \exp(-P_e))/2)}{P_e(1 - \exp(-P_e))^2/2} \tag{28}$$

One can obtain similar expressions for the case $u < 0$.

REFERENCES

1. K. Barrett, 'Super upwinding—elements of doubt and discrete differences of opinion on the numerical muddling of the incomprehensible defective confusion equation', *Numerical Modelling in Diffusion Convection*, J. Caldwell and A. O. Moscardini, Editors, Pentech Press, 1982.
2. D. B. Spalding, 'A novel finite difference formulation for differential expressions involving both first and second derivatives', *Int. J Num. Meth. Eng.*, **4**, 557–559 (1972).
3. B. P. Leonard, 'Newsflash: upstream parabolic interpolation', *Proc. 2nd GAMM Conference on Numerical Methods in Fluid Mechanics*, Koln, W. Germany.
4. B. P. Leonard, 'Third-order finite-difference method for steady two-dimensional convection', *Num. Meth. in Laminar and Turbulent Flow*, 807–819 (1978).

5. D. B. Spalding, 'A general purpose computer program for multidimensional one- and two-phase flow', *Mathematics and Computers in Simulation*, **XXIII,** 267–276 (1981).
6. N. C. Markatos, A. Moult, P. J. Phelps and D. B. Spalding, 'The calculation of steady, three-dimensional, two-phase flow and heat transfer in steam generators'. *Proc. ICHMT Seminar.* Dubrovnik, Yugoslavia, Hemisphere, pp. 485–502 (1978).
7. N. C. Markatos and D. Kirkcaldy, 'Analysis and computation of three-dimensional, transient flow and combustion through granulated propellants', *Int. J. Heat Mass Transfer*, **26,** (7), 1037–1053 (1983).
8. G. D. Raithby, 'Skew upstream differencing schemes for problems involving fluid flow', *Comp. Methods in Applied Mech. and Eng.*, **9,** 153–164 (1976).
9. G. D. Raithby, 'A critical evaluation of upstream differencing applied to problems involving fluid flow', *Comp. Methods in Applied Mech. and Eng.*, **9,** 75–103 (1976).
10. A. Pollard and Alan L. W. Siu, 'The calculation of some laminar flows using various discretisation schemes', *Comp. Methods in Applied Mech. and Eng.*, **35,** 293–313 (1982).
11. S. V. Patankar, *Numerical Heat Transfer and Fluid Flow*, McGraw-Hill, New York, 1980.
12. B. P. Leonard, 'A stable and accurate convective modelling procedure based on quadratic upstream interpolation', *Comp. Methods in Applied Mech. and Eng.*, **19,** 59–98 (1979).
13. S. V. Patankar and D. B. Spalding, 'A calculation procedure for heat, mass and momentum transfer in three-dimensional parabolic flows', *Int. J. Heat Mass Transfer.*, **15,** 1787–1806 (1972).
14. T. Han and J. A. C. Humphrey, 'A comparison of hybrid and quadratic-upstream differencing in high Reynolds number elliptic flows', *Comp. Methods in Applied Mech. and Eng.*, **29,** 81–95 (1981).
15. D. S. Conte and C. de Boor, *Elementary Numerical Analysis. An Algorithmic Approach*, McGraw-Hill, New York, 1980.